



Dalton
Transactions

Tris-(2-pyridylmethyl)amine-ligated Cu(II) 1,3-diketonate complexes: Anaerobic retro-Claisen and dehalogenation reactivity of 2-chloro-1,3-diketonate derivatives

Journal:	<i>Dalton Transactions</i>
Manuscript ID	DT-ART-11-2020-004074.R1
Article Type:	Paper
Date Submitted by the Author:	05-Jan-2021
Complete List of Authors:	Elsberg, Josiah; Utah State University, Chemistry Anderson, Stephen; Utah State University, Chemistry Tierney, David; Miami University Reinheimer, Eric; Rigaku Americas Berreau, Lisa; Utah State University, Department of Chemistry

SCHOLARONE™
Manuscripts

ARTICLE

Tris-(2-pyridylmethyl)amine-ligated Cu(II) 1,3-diketonate complexes: Anaerobic retro-Claisen and dehalogenation reactivity of 2-chloro-1,3-diketonate derivatives

Received 00th January 20xx,
Accepted 00th January 20xx

DOI: 10.1039/x0xx00000x

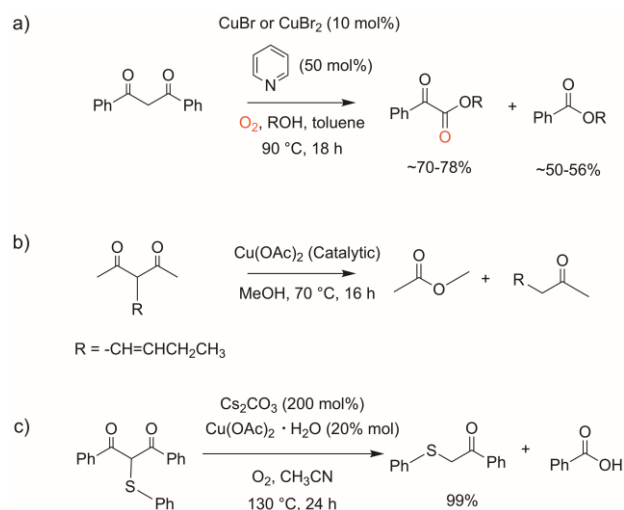
Josiah G. D. Elsberg,^a Stephen N. Anderson,^a David L. Tierney,^b Eric W. Reinheimer^c and Lisa M. Berreau^{a*}

We report synthetic, structural and reactivity investigations of tris-(2-pyridylmethyl)amine (TPA)-ligated Cu(II) 1,3-diketonate complexes. These complexes exhibit anaerobic retro-Claisen type C-C bond cleavage reactivity which exceeds that found in analogs supported by chelate ligands with fewer and/or weaker pyridyl interactions.

Introduction

Aliphatic carbon-carbon (C-C) bond cleavage reactions of 1,3-diketones mediated by copper salts are of current interest.^{1,2} In applications for organic synthesis, reports have appeared of oxidative cleavage of dibenzoylmethane and other 1,3-diketones using CuBr or CuBr₂ under air with excess pyridine (5 eq) present as a supporting ligand (Scheme 1(a)) and with prolonged heating.^{3,4} For the most part, the mechanistic pathways of these reactions remain undefined, as does the influence that pyridine ligation has on possible intermediates. Non-redox reactions involving retro-Claisen-type aliphatic C-C bond cleavage reactivity of 1,3-diketones mediated by Cu(II) salts have also been reported.⁵⁻⁷ Similar to Cu(II)-mediated oxidative diketone cleavage (Scheme 1(a)), these reactions typically involve undefined Cu(II) diketone/diketonate species under prolonged high temperature conditions (>80 °C) (Scheme 1(b) and (c)) in the presence of water or alcohol.

We hypothesize that insight into the chemical factors that influence copper-mediated oxidative and non-redox 1,3-diketone cleavage can be gained through studies involving copper complexes supported by pyridyl-containing chelate ligands. In this regard, our laboratory has previously reported



Scheme 1. Aliphatic C-C bond cleavage reactions mediated by copper salts.

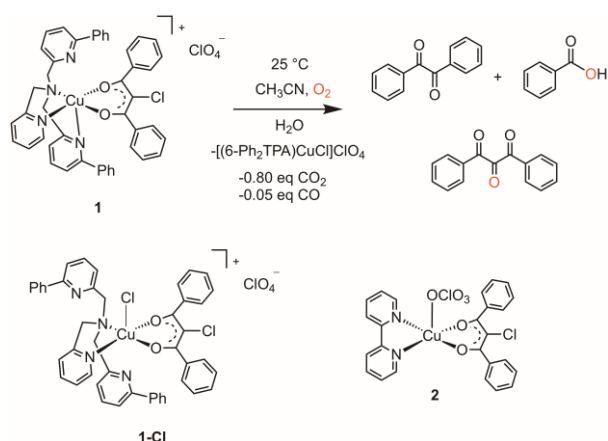
studies of the oxidative aliphatic C-C bond cleavage reactivity of a Cu(II) chlorodiketonate complex (**1**, Scheme 2) supported by the 6-Ph₂TPA ligand.^{8,9} Notably, chloride anion binding to the Cu(II) center in this complex lowers the barrier for O₂ activation, providing evidence for the importance of the primary coordination sphere in influencing oxidative diketone cleavage reactivity. In the solid state, the Cu(II) center of **1** exhibits coordination to the tertiary amine nitrogen (Cu(II)-N_{am} 2.0333(17) Å) and the unsubstituted pyridyl donor (Cu(II)-N_{py} 1.992(18) Å) of the chelate ligand, with one phenyl-appended pyridyl donor interacting more weakly (Cu(II)-N_{PhPy} 2.3394(18) Å). The remaining aryl-appended pyridine appendage of the chelate ligand is dissociated from the Cu(II) center. The EPR spectral features of **1** provide evidence for the retention of this five-coordinate structure in frozen acetonitrile.⁸ DFT modelling of the chloride-activated **1-Cl** (Scheme 2) suggests formation of a square-pyramidal structure with chloride binding in the axial position and loss of the Cu(II)-N_{PhPy} interaction. Consistent with

^a Department of Chemistry & Biochemistry, Utah State University, 0300 Old Main Hill, Logan, UT 84322-0300 USA

^b Department of Chemistry & Biochemistry, Miami University, Oxford, OH 45056 USA

^c Rigaku Americas Corporation, 9009 New Trails Drive, The Woodlands, TX 77381 USA

*Electronic Supplementary Information (ESI) available: Experimental details and spectral data; crystallographic data: CCDC 2010712 2010713 2010714 2010715 2010716 2038517. See DOI: 10.1039/x0xx00000x



Scheme 2. (top) Oxidative aliphatic C-C bond cleavage reactivity of **1**. (bottom) Structures of **1-Cl** and **2**.

the proposed structure of **1-Cl**, a bipyridine-coordinated analog **2** also exhibits chloride-activated oxidative C-C bond cleavage reactivity.⁹

Based on the chloride- and O_2 -dependent C-C bond cleavage reactivity exhibited by **1** and **2**, we hypothesized that increasing the donor properties of the pyridyl-containing chelate ligand would potentially limit anion binding to the Cu(II) center and O_2 activity. To probe this idea, we targeted for synthesis and reactivity studies two series of tris(2-pyridylmethyl)amine (TPA)-ligated Cu(II) 1,3-diketonate complexes. The first set of complexes, formulated as $[(\text{TPA})\text{Cu}(4'\text{-R-PhC}(\text{O})\text{CHC}(\text{O})4'\text{-R-Ph})]\text{ClO}_4$ (**3-6**, R = -H, - CH_3 , - OCH_3 , -Cl) contain a diketonate that is unsubstituted at the central position. Our hypothesis was that these complexes would be air stable and provide benchmark examples of rare pseudo-octahedral Cu(II) diketonate complexes. The second set of complexes targeted for synthesis were TPA-ligated Cu(II) chlorodiketonate derivatives, $[(\text{TPA})\text{Cu}(4'\text{-R-PhC}(\text{O})\text{CCIC}(\text{O})4'\text{-R-Ph})]\text{ClO}_4$ (**7-10**, R = -H, - CH_3 , - OCH_3 , -Cl). Notably, we have found that using the synthetic conditions employed to generate **1** and **2** under N_2 in attempts to make **7-10** leads to both retro-Claisen type aliphatic C-C bond cleavage reactivity and dehalogenation of the chlorodiketonate ligand. We report herein comprehensive characterization details for **3-6** as well as a series of experiments to probe the retro-Claisen and dehalogenation reactivity identified in the anaerobic reactions directed at the preparation of **7-10**. Overall, the results presented herein demonstrate that the pyridyl donor characteristics of a supporting ligand significantly influence the structure and reactivity of Cu(II) chlorodiketonate species.

Experimental

General Methods. All solvents and reagents were purchased from commercial sources and used without prior purification unless otherwise stated. Solvents were dried following a previously published procedure and distilled under N_2 prior to use.¹⁰ Tris(2-pyridylmethyl)amine (TPA)¹¹, *N,N*-bis((6-phenyl-2-pyridyl)methyl)-*N*-((2-pyridyl)methyl)amine (6- Ph_2TPA)¹², 1,3-bis(4'-R-phenyl)-1,3-

propanediones¹³, 2-chloro-1,3-bis(4'-R-phenyl)-1,3-propanedione¹⁴, 2-chloro-1-(4'-R-phenyl)ethanone¹⁴, $[(\text{TPA})\text{Cu}(\text{CH}_3\text{CN})](\text{ClO}_4)_2$ ¹⁵ and $[(\text{TPA})\text{Cu}(\text{CH}_3\text{CN})]\text{PF}_6$ ¹¹ were prepared according to literature procedures. All manipulations involving the preparation of Cu(II) complexes were performed in an MBraun Unilab glovebox under a N_2 atmosphere unless otherwise noted.

Physical Methods. ^1H and ^{13}C NMR spectra of diamagnetic compounds were collected using a Bruker Advance III HD Ascend-500 spectrometer. Chemical shifts (ppm) are reported relative to the residual solvent peak in CD_2HCN (^1H NMR: 1.94 ppm, quintet) or CHCl_3 (^1H NMR: 7.26 ppm, singlet). FTIR spectra were collected as KBr pellets using a Shimadzu FTIR-8400 spectrometer. UV-vis data was collected on a Hewlett-Packard 8453A diode array spectrometer at ambient temperature. ESI mass spectral data were collected using a Shimadzu LCMS-2020. Elemental analyses were performed by Robertson Microlit Laboratories (Ledgewood, N.J.) or Atlantic Microlab (Norcross, GA).

Caution! Perchlorate compounds containing organic ligands are potentially explosive. These materials should be handled with care and in small quantities.¹⁶

Synthesis of 2-Chloro-1,3-bis(4'-chlorophenyl)-1,3-propanedione.

1,3-bis(4'-chlorophenyl)-1,3-propanedione (2.04 mmol) was dissolved in MeOH (80 mL) and ammonium chloride (4.08 mmol) and OXONE® (3.07 mmol) were added. The solution was refluxed for 5 h and then stirred for an additional 12 h at ambient temperature. Following addition of H_2O (30 mL) the volume of the solution was reduced using rotary evaporation. Water (20 mL) and EtOAc (20 mL) were added and the solution transferred to a separatory funnel. The organic layer was collected, and the aqueous phase was extracted with two additional aliquots of EtOAc (2 x 20 mL). The combined organic fractions were dried over Na_2SO_4 , the solution filtered, and the solvent from the filtrate was then removed by rotary evaporation. The resulting solid was dissolved in a minimal amount of hot EtOH and then placed in the freezer (-12°C) for 16 h which resulted in the deposition of a white solid. (0.26 g, 40%). mp $124\text{-}125^\circ\text{C}$, ^1H NMR (CDCl_3) δ (ppm): 7.94 (m, $J = 8.7$ Hz, 4H), 7.45 (m, $J = 8.7$ Hz, 4H), 6.25 (s, 1H). ^{13}C NMR (CDCl_3) δ (ppm): 188.4 (C=O), 141.4, 132.2, 131.0, 129.6, 63.5 (6 signals expected and observed). FTIR (KBr, cm^{-1}): 1702($\nu_{\text{C=O}}$), 1680, 1587.

General Synthesis of $[(\text{TPA})\text{Cu}(4'\text{-R-PhC}(\text{O})\text{CHC}(\text{O})4'\text{-R-Ph})]\text{ClO}_4$ (3-6**).** Under an inert atmosphere at $\sim 30^\circ\text{C}$, $\text{Cu}(\text{ClO}_4)_2 \cdot 6\text{H}_2\text{O}$ (0.135 mmol) was dissolved in CH_3CN (~ 3 mL) and added to solid TPA (0.135 mmol). The resulting deep blue solution was stirred for 30 min. In a separate container, 1,3-(4'-R-phenyl)-1,3-propanedione (R = -H, - CH_3 , - OCH_3 , -Cl) (0.135 mmol) was combined with lithium bis(trimethylsilyl)amide (0.135 mmol) dissolved in Et_2O (~ 3 mL) and stirred for 5 min. In all cases, this produced a murky solution containing an insoluble white precipitate. The two solutions were then combined and stirred for an hour, resulting in the formation of a green reaction

mixture. The solvent was then removed under reduced pressure and the residual solid was dissolved in CH_2Cl_2 . This solution was passed through a celite plug and the eluent was brought to dryness under vacuum. Crystals suitable for X-ray diffraction were grown by vapor diffusion of Et_2O into a CH_2Cl_2 solution of **3-6**. Yields and characterization data are stated below:

[(TPA)Cu(PhC(O)CHC(O)Ph)] ClO_4 (**3**): (22 mg, 22%). Anal. calc. for $\text{C}_{33}\text{H}_{29}\text{ClCuN}_4\text{O}_6$: C, 58.58; H, 4.32; N, 8.28. Found: C, 58.52; H, 4.17; N, 7.85. ESI-MS: m/z calc. for $\text{C}_{33}\text{H}_{29}\text{CuN}_4\text{O}_2$, 576.2 [M- ClO_4] $^+$; found 576.3 [M- ClO_4] $^+$. UV-vis (CH_3CN) λ_{max} , nm (ϵ , $\text{M}^{-1}\text{cm}^{-1}$): 356 (16270). FT-IR (KBr, cm^{-1}): 1600, 1550, 1520, 1380, 1090(ν_{ClO_4}), 630(ν_{ClO_4}).

[(TPA)Cu(4'- CH_3 -PhC(O)CHC(O)4'- CH_3 -Ph)] ClO_4 (**4**): (27 mg, 29%). Anal. calc. for $\text{C}_{35}\text{H}_{33}\text{ClCuN}_4\text{O}_6 \cdot 0.1\text{CH}_2\text{Cl}_2$: C, 59.11; H, 4.69; N, 7.86. Found: C, 58.89; H, 4.51; N, 7.85. ESI-MS: m/z calc. for $\text{C}_{35}\text{H}_{33}\text{CuN}_4\text{O}_2$, 604.2 [M- ClO_4] $^+$; found 604.3 [M- ClO_4] $^+$. UV-vis (CH_3CN) λ_{max} , nm (ϵ , $\text{M}^{-1}\text{cm}^{-1}$): 360 (18230). FT-IR (KBr, cm^{-1}): 1590, 1530, 1370, 1090(ν_{ClO_4}), 620(ν_{ClO_4}).

[(TPA)Cu(4'- OCH_3 -PhC(O)CHC(O)4'- OCH_3 -Ph)] ClO_4 (**5**): (34 mg, 35%). Anal. calc. for $\text{C}_{35}\text{H}_{33}\text{ClCuN}_4\text{O}_8 \cdot 0.2\text{CH}_2\text{Cl}_2$: C, 56.10; H, 4.47; N, 7.43. Found: C, 55.76; H, 4.19; N, 7.43. ESI-MS: m/z calc. for $\text{C}_{35}\text{H}_{33}\text{CuN}_4\text{O}_4$, 636.2 [M- ClO_4] $^+$; found 636.3 [M- ClO_4] $^+$. UV-vis (CH_3CN) λ_{max} , nm (ϵ , $\text{M}^{-1}\text{cm}^{-1}$): 367 (22030). FT-IR (KBr, cm^{-1}): 1600, 1530, 1370, 1260, 1180, 1090(ν_{ClO_4}), 620(ν_{ClO_4}).

[(TPA)Cu(4'- Cl -PhC(O)CHC(O)4'- Cl -Ph)] ClO_4 (**6**): (12 mg, 12%). Anal. calc. for $\text{C}_{33}\text{H}_{27}\text{Cl}_3\text{CuN}_4\text{O}_6$: C, 53.17; H, 3.65; N, 7.52. Found: C, 53.48; H, 3.61; N, 7.50. ESI-MS: m/z calc. for $\text{C}_{33}\text{H}_{27}\text{Cl}_2\text{CuN}_4\text{O}_2$, 644.1 [M- ClO_4] $^+$; found 644.1 [M- ClO_4] $^+$. UV-vis (CH_3CN) λ_{max} , nm (ϵ , $\text{M}^{-1}\text{cm}^{-1}$): 363 (19650). FT-IR (KBr, cm^{-1}): 1589, 1530, 1365, 1093(ν_{ClO_4}), 626(ν_{ClO_4}).

Attempted Syntheses of [(TPA)Cu(4'-R-PhC(O)CCIC(O)4'-R-Ph)] ClO_4 (7-10**).** Under an inert atmosphere at $\sim 30^\circ\text{C}$, $\text{Cu}(\text{ClO}_4)_2 \cdot 6\text{H}_2\text{O}$ (0.135 mmol) was dissolved in CH_3CN (~ 3 mL) and added to solid TPA (0.135 mmol). The resulting deep blue solution was stirred for 30 min. In a separate vial, 2-chloro-1,3-(4'-R-phenyl)-1,3-propanedione (R = -H, - CH_3 , - OCH_3 , -Cl) (0.135 mmol) was combined with lithium bis(trimethylsilyl)amide (0.135 mmol) dissolved in Et_2O (~ 3 mL) and the resulting mixture was stirred for 5 min. This produced a yellow solution containing an insoluble precipitate for all derivatives. The solutions were then combined and stirred overnight (16 h), resulting in the formation of a clear green solution. Difficulties in producing analytically pure crystalline products led us to collect ESI-MS data for each final reaction mixture. This data indicated the presence of the following ions: [(TPA)Cu(4'-R-PhC(O)CCIC(O)4'-R-Ph)] $^+$, [(TPA)Cu(4'-R-PhC(O)CHC(O)4'-R-Ph)] $^+$, [(TPA)Cu(O_2C -4'-R-Ph)] $^+$ and [(TPA)CuCl] $^+$. These ions suggested aliphatic C-C bond cleavage reactivity and dehalogenation within the diketonate moiety under anaerobic conditions. Notably, attempted crystallization of **9** resulted in the deposition of crystals of the dehalogenated product **5** and [(TPA)Cu-Cl] $_2$ [Li(ClO_4) $_3$]. (**11**)

Independent Synthesis of [(TPA)Cu(O_2CPh)] ClO_4 (12**).** Under an inert atmosphere at $\sim 30^\circ\text{C}$, $\text{Cu}(\text{ClO}_4)_2 \cdot 6\text{H}_2\text{O}$ (0.0675 mmol) dissolved in CH_3CN (~ 3 mL) and added to solid TPA (0.0675 mmol). The resulting deep blue solution was stirred for 30 min. This solution was then added to a vial containing solid sodium benzoate (0.0675 mmol). Following addition of methanol sufficient to produce a homogenous mixture, the solution was stirred overnight (16 h). After removal of the solvent under reduced pressure, the remaining solid was dissolved in CH_2Cl_2 (~ 3 mL), and the solution passed through a celite plug. The filtrate was collected and brought to dryness under reduced pressure. Crystals suitable for X-ray diffraction were grown by vapor diffusion of Et_2O into a solution of **12** dissolved in 1:1 $\text{CH}_3\text{CN}:\text{CH}_2\text{Cl}_2$. Yield: 18.1 mg (47%). Anal. calc. $\text{C}_{25}\text{H}_{23}\text{ClCuN}_4\text{O}_6 \cdot 0.6\text{CH}_2\text{Cl}_2$: C, 49.16; H, 3.90; N, 8.96. Found: C, 49.08; H, 3.70; N, 8.95. ESI-MS: m/z calc. for $\text{C}_{25}\text{H}_{23}\text{CuN}_4\text{O}_2$, 644.1 [M- ClO_4] $^+$; found 644.1 [M- ClO_4] $^+$.

Organic Product Isolation from Reaction Mixtures of **7-10.** To gain insight into the anaerobic diketonate cleavage and dehalogenation reactivity occurring in the reaction mixtures of **7-10** the organic products of each reaction were isolated and characterized. Under an inert atmosphere in a N_2 -filled glovebox at $\sim 30^\circ\text{C}$, $\text{Cu}(\text{ClO}_4)_2 \cdot 6\text{H}_2\text{O}$ (0.0675 mmol) was dissolved in CH_3CN (~ 2 mL) and added to solid TPA (0.0675 mmol). The deep blue solution was stirred for approximately 30 min. In a separate vial, 2-chloro-1,3-bis(4'-R-phenyl)-1,3-propanedione (R = -H, - CH_3 , - OCH_3 , -Cl) (0.0675 mmol) was combined with lithium bis(trimethylsilyl)amide (0.0675 mmol) in Et_2O (~ 2 mL). This solution was stirred for 5 min, producing a yellow mixture with insoluble precipitate for all derivatives. The solutions were then combined and stirred for 48 hr. One equivalent of triphenylmethane (Ph_3CH) was then added as an internal standard and the solvent removed under reduced pressure. The solid residue was removed from the glovebox, dissolved in ethyl acetate and passed through a silica plug. The eluent was dried over anhydrous sodium sulfate and the solvent removed by rotary evaporation. The remaining solid was dissolved in CDCl_3 and the ^1H NMR spectrum obtained. The retro-Claisen 2-chloro-1-(4'-R-phenyl)ethanone products were identified by comparison of spectral features to analytically pure samples that had been independently prepared.¹⁷ Quantification of each 2-chloro-1-(4'-R-phenyl)ethanone derivative was achieved via integration of its methylene resonance versus the methine proton resonance at 5.55 ppm (relative to CDCl_3) of the Ph_3CH internal standard. Control experiments and examples involving excess H_2O (200 eq) were performed in a similar manner.

Organic Product Recovery from the Attempted Synthesis of **7 Under Conditions Wherein the Amount of Water is Varied.** To probe the role of water in the retro-Claisen reactivity identified in the attempted preparation of **7**, under an inert atmosphere, [(TPA)Cu(CH_3CN)](ClO_4) $_2$ (0.0675 mmol) was dissolved in dry CH_3CN (~ 2 mL) and the solution was stirred for ~ 5 min. In a separate vial, 2-chloro-1,3-diphenyl-1,3-propanedione (0.0675 mmol) was combined with lithium bis(trimethylsilyl)amide

(0.0675 mmol) in Et₂O (~2 mL) and stirred for 5 min, producing a yellow solution with an insoluble precipitate. These solutions were then combined resulting in the formation of a green solution that was stirred for 48 hr. The internal standard Ph₃CH (1 eq) was added and the solvent removed under reduced pressure. The organic extraction procedure involving ethyl acetate described above was then used to isolate the organic products. Controls involving excess (200 eq) H₂O, D₂O and MeOH were performed the same way, except each was added 30 minutes after the reaction had started.

Dehalogenation Reactivity of 2-chloro-1,3-bis(4'-phenyl)-1,3-propanedione Mediated by [(TPA)Cu(CH₃CN)]PF₆. Under an inert atmosphere, [(TPA)Cu(CH₃CN)]PF₆ (0.02 mmol) was dissolved in a mixture of CH₃CN/Et₂O (1:1; 3 mL). The resulting yellow solution was added to solid 2-chloro-1,3-diphenyl-1,3-propanedione (0.02 mmol) which resulted in the formation of a green solution. After stirring for 1 h, the solvent was removed under reduced pressure. The remaining solid was removed from the glovebox, dissolved in HCl (8 mL, 1M) and CH₂Cl₂ (8 mL), and stirred for 1 h. The organic layer was separated, dried over sodium sulfate and subsequently filtered. The filtrate was collected and brought to dryness under reduced pressure using a rotary evaporator. ¹H NMR analysis of the yellow solid showed a 1:1 mixture of 1,3-diphenyl-1,3-propanedione and unreacted 2-chloro-1,3-bisphenyl-1,3-propanedione. Repeating the reaction with two equivalents of [(TPA)Cu(CH₃CN)]PF₆ revealed the formation of 1,3-diphenyl-1,3-propanedione as the primary product (89%).

EPR Spectroscopy. Low-temperature X-band EPR of **3-5** were acquired on a Bruker EMX EPR spectrometer equipped with a DM-4116 dual mode resonator and an Oxford instruments ESR-900 cryostat and temperature controller. Spectra were collected at 4.5 K on samples that were ~3 mM in 50/50 dichloromethane/toluene. Other spectrometer settings: ν_{MW} = 9.62 GHz (2 μ W); time constant/conversion time = 42 ms; modulation amplitude 2 G (100 kHz); receiver gain = 10⁵; 4 scans. The EPR spectra were simulated using EasySpin run within MatLab. All of the simulations presented used a 25 G Gaussian line shape with other parameters as noted in the text. Low temperature X-band EPR spectra of **6** and reactions mixtures for **7-10** were acquired on a Bruker EMX EPR spectrometer with an OxfordITC503 liquid helium cryostat. The spectra were collected at 12 K on samples that were ~3 mM in 1:1 acetonitrile/toluene. Other spectrometer settings: ν_{MW} = 9.38 GHz (20 μ W); time constant/conversion time = 21 ms; modulation amplitude 8 G (100 kHz); receiver gain = 10⁴; 10 scans.

X-Ray Crystallography. Single crystals of **3-6**, **11** and **12** were used for X-ray crystallography studies. Structures for **3**, **4**, **11** and **12** were determined at the University of Montana (UM) wherein a crystal of each was mounted on a glass fiber loop using viscous oil and transferred to a Bruker D8 Venture using MoK α (λ =0.71073 Å) radiation for data collection at 100 K. The structure of **5** was determined by Rigaku, wherein a single

crystal was mounted on a glass fiber using viscous oil and transferred to a XtaLAB Synergy-S using MoK α (λ =0.71073 Å) radiation for data collection at 100 K. The structure of **6** was determined at Utah State University, wherein a single crystal of **6** was mounted on a glass fiber loop using viscous oil and transferred to a Rigaku XtaLAB Mini II Diffractometer using MoK α (λ = 0.71073 Å) radiation for data collection at 100 K.

Data were corrected for absorption using SADABS¹⁷ (**3**, **4**, **11** and **12**) or Gaussian grid (numerical integration) (**5** and **6** with **6** having a 0.5 mm 1D horizontal Gaussian beam correction for the graphite monochromator). Using Olex2¹⁸, the structure of each complex was solved with the SHELXT¹⁹ structure solution program using direct methods and refined with the SHELXL²⁰ refinement package using least square minimization. All non-hydrogen atoms were refined with anisotropic thermal parameters. Hydrogen atoms in each structure (except for the acetonitrile in **11**) were placed in geometrically calculated positions and refined using a riding model. Isotropic thermal parameters of all hydrogen atoms were fixed to 1.2 times the *U* value of the atoms they are linked to (1.5 times for methyl groups). Calculations and refinement of structures were carried out using APEX2²¹ for **3** and **12** (APEX3²² for **4** and **11**), SHELXTL¹⁹, and Olex2¹⁸ software. For **5** and **6**, calculations and refinement of structures were carried out using CrysAlisPro²³, SHELXL²⁰, and Olex2¹⁸ software.

3. The perchlorate anion in **3** was modelled over two positions using a PART instruction and tied to a single free variable. Refinement of the free variable shows an approximate 67:33 disorder. Thermal ellipsoid constraints and similarity restraints (EADP and SADI) were used to model the disorder. The structure presented some difficulties in space group determination. Violations of systematic absences lead to a discrepancy between two monoclinic space groups *P*21 or *P*21/*c*. The reflections violating the symmetry element conditions for the *P*21/*c* are weak, suggesting that possible disorder, a satellite crystal, or a small contributing twin could be causing this observation. Multiple data sets were collected although the weak reflections violating systematic absences persisted. Therefore, the data were solved (and refined) in both space group settings and compared. The centrosymmetric *P*21/*c* resulted in a higher R1 statistic than the *P*21 model however, this is not a valid reason to pick one model over the other. Geometrical parameters for the *P*21/*c* model produced better statistics than the *P*21 model when compared to structures in Cambridge Structural Database using the Cambridge Crystallographic Data Centre program Mogul²⁴ and Mercury²⁵. Considering the better geometrical model and the relatively weak reflections violating the systematic absences the centrosymmetric *P*21/*c* model was chosen.

6. After anisotropic refinement of non-hydrogen atoms and H placement, the flack parameter was calculated at 0.517. A twin law

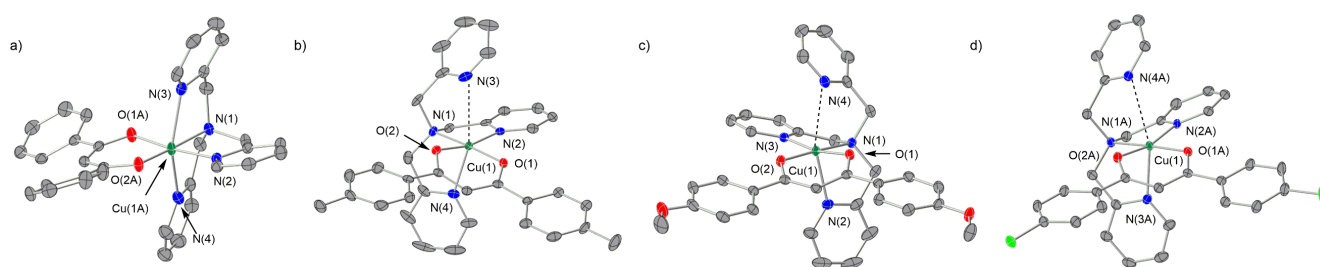
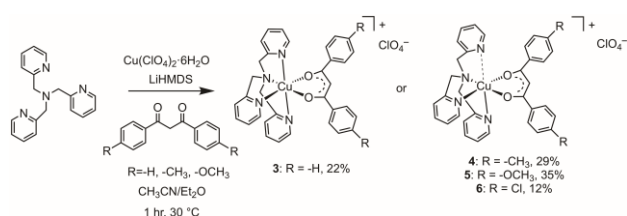


Figure 1. Representations of the cationic portions of the X-ray structures of **3** (a), **4** (b), **5** (c), and **6** (d). Ellipsoids are plotted at the 50% probability level. Only one of two similar cations found in the asymmetric units of **3** and **6** are shown. Hydrogen atoms have been omitted for clarity.

of $(-1, 0, 0, 0, -1, 0, 0, 0, -1)$ was introduced for the subsequent refinements along with the calculation of a batch scale factor (BASF). Additionally, a solvent mask was calculated, and 6 electrons were found in a volume of 32 \AA^3 in 1 void per unit cell. This is consistent with the presence of one $\text{CH}_3\text{CH}_2\text{OCH}_2\text{CH}_3$ per asymmetric unit which accounts for 84 electrons per unit cell.



Scheme 3. Synthesis of **3-6**.

Results and Discussion

Synthesis and Characterization of TPA-ligated Cu(II) Diketonate Complexes 3-6. The series of complexes $[(\text{TPA})\text{Cu}(4'\text{-R-PhC}(\text{O})\text{CHC}(\text{O})4'\text{-R-Ph})]\text{ClO}_4$ ($\text{R} = \text{-H}$ (**3**), -CH_3 (**4**), -OCH_3 (**5**), -Cl (**6**)) was synthesized (Scheme 3) and isolated in crystalline form. Each complex was characterized by elemental analysis, X-ray crystallography, EPR, UV-Vis, ESI-MS and FT-IR (Figures S1-S15). The cation of **3** (Figure 1(a)) exhibits a six-coordinate Cu(II) center with two axially coordinated N_{py} donors with Cu-N distances of $\sim 2.3 \text{ \AA}$ and equatorial N_{am} and N_{py} donors at 2.10 and 2.01 \AA , respectively. The cationic portions of **4-6** (Figure 1(b)-1(d)) which have electron donating (**4**, **5**) or withdrawing (**6**) substituents on the diketonate ligand, exhibit a more distorted geometry with one weak axial Cu- N_{py} interaction ($>2.75 \text{ \AA}$). While variation is found in the axial Cu- N_{py} interactions, **3-6** exhibit similar equatorial Cu(II)- N_{am} and Cu- N_{py} distances (2.043-2.062 \AA and 1.982-1.994 \AA , respectively) to those found in **3**. Both oxygen donors of the diketonate ligand lie in the equatorial plane in **3-6**, with Cu(II)-O distances in the range of 1.923-1.947 \AA .

Frozen CH_2Cl_2 :toluene (1:1) solutions of **3-5** examined at 4.5 K exhibit similar EPR spectral features that are consistent with a highly axial Cu(II) center (Figure 2). Attempts to simulate the spectral features required the inclusion of both the $^{63,65}\text{Cu}$

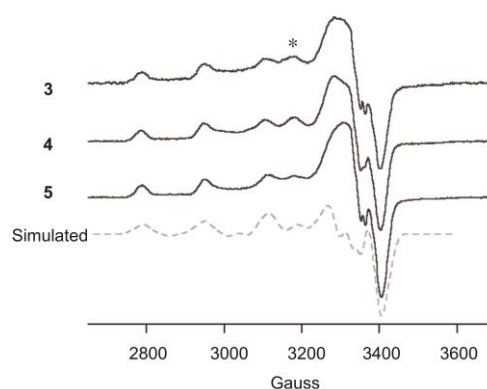


Figure 2. EPR spectra of **3-5** in CH_2Cl_2 :toluene (1:1) at 4.5 K and a simulated spectrum. For **3-5**, $g_{\parallel} = 2.27$, $g_{\perp} = 2.06$, and $^{63,65}\text{Cu}$ couplings of $[A_{\parallel}, A_{\perp}] = [510, 60] \text{ MHz}$.

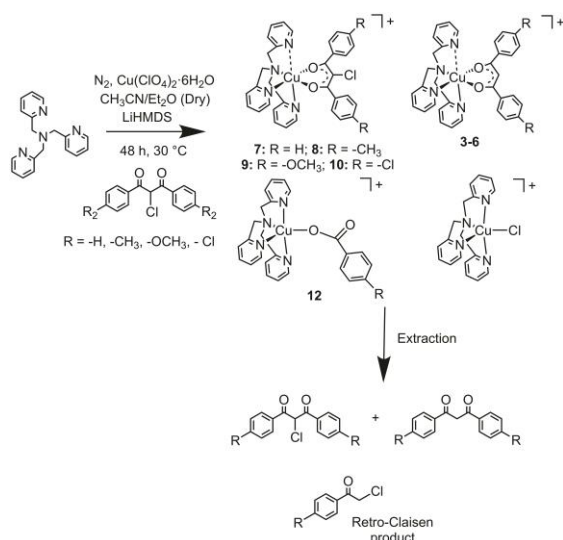
hyperfine couplings and the hyperfine couplings of all four TPA-derived ^{14}N donors. $^{63,65}\text{Cu}$ couplings of $[A_{\parallel}, A_{\perp}] = [510, 60] \text{ MHz}$ with $[g_{\parallel}, g_{\perp}] = [2.27, 2.06]$ reproduce nearly all of the salient features of this spectrum, with the exception of the signal at $\sim 3180 \text{ G}$ (marked with an asterisk in Figure 2). The pattern of ^{14}N hyperfine couplings suggests that two of the pyridine nitrogen atoms define g_{\parallel} ($[A_{\parallel}, A_{\perp}] = [40, 20]$), with the other pyridine nitrogen ($[A_{\parallel}, A_{\perp}] = [20, 40]$) and the tertiary amine ($[A_{\parallel}, A_{\perp}] = [40, 40]$) lying in the xy -plane (Figure S1). The EPR spectrum of **6** collected at 12 K in frozen CH_3CN :toluene (1:1) contains similar features (Figure S2).

The absorption spectra of **3-6** dissolved in CH_3CN contain a π - π^* band at ~ 355 -370 nm (Figures S3-S7). Exposure of solutions of **3-6** to air over 12 h produced no change in the absorption features, consistent with the complexes being air stable. ESI-MS spectra show the expected molecular ion cluster for $[(\text{TPA})\text{Cu}(4'\text{-R-PhC}(\text{O})\text{CHC}(\text{O})\text{Ph-4'-R})]^+$ for **3-6** (Figures S8-S11) as well as a cluster for the $[(\text{TPA})\text{Cu-Cl}]^+$ ion may be appearing as a result of perchlorate reduction in the mass spectrometer. FTIR spectra of **3-6** collected as KBr pellets are provided in Figures S12-S15.

Overall, **3-6** represent rare examples of structurally characterized six coordinate Cu(II) diketonate complexes. TPA-ligation differentiates **3-6** from **1** which exhibits a five-coordinate Cu(II) center due to the weaker donation of a phenyl-appended pyridyl donor.

Anaerobic Reactivity of TPA-ligated Cu(II) Chlorodiketonate Complexes. We next targeted for synthesis a series of Cu(II) chlorodiketonate complexes with the eventual goal of examining their reactivity with O₂ for comparison to the reactivity of **1** (Scheme 2). Following the synthetic procedure outlined in Scheme 3 for the preparation of **7-10** under N₂ we found that a mixture of products was generated. This initially became evident when we attempted to crystallize the R = -OCH₃ derivative **9** and obtained X-ray quality crystals of [(TPA)Cu(4'-OCH₃-PhC(O)CHC(O)4'-OCH₃-Ph)]ClO₄ (**5**) and [(TPA)Cu-Cl]₂[Li(ClO₄)₃] (**11**) (Figure S16). The isolation of these complexes provides evidence for dehalogenation reactivity. We subsequently investigated each reaction mixture using ESI-MS. In the attempted synthesis of the parent complex, [(TPA)Cu(PhC(O)C(Cl)C(O)Ph)]ClO₄ (**7**), isotope clusters were identified for the desired product [(TPA)Cu(PhC(O)CCIC(O)Ph)]⁺ (*m/z* 610.2) along with clusters for [(TPA)Cu(PhC(O)CHC(O)Ph)]⁺ (*m/z* 576.3), [(TPA)CuCl]⁺ (*m/z* 388.1) and [(TPA)Cu(O₂CPh)]⁺ (*m/z* 474.2) (Figure S17). Thus, in addition to the dehalogenation reactivity noted above, the formation of the benzoate cluster also provided evidence for aliphatic C-C bond cleavage reactivity. [(TPA)Cu(O₂CPh)]ClO₄ (**12**) was independently synthesized and characterized by X-ray crystallography (Figure S18) and ESI-MS (Figure S19) to support the formulation of this carboxylate product. Similar ESI-MS reaction mixtures were found for the methyl-, methoxy- and chloro-substituted chlorodiketonate derivatives (Figures S20-S22).

To gain further insight into the reaction mixtures of **7-10**, the free organic products in each were isolated via drying of the mixture under reduced pressure followed by extraction using



Scheme 4. Aliphatic C-X and C-C bond cleavage reactivity identified in anaerobic reaction mixtures directed at the synthesis of TPA-ligated Cu(II) chlorodiketonate complexes.

ethyl acetate in the presence of an internal standard (CHPh₃) (Scheme 4). ¹H NMR analysis of the organics revealed the presence of a 4'-R-chloroacetophenone derivative in 17-31% yield depending on the chlorodiketonate substituent (Table 1, entries 1-4; Figure S23-S26). Addition of excess water (200 eq) more than doubled the yield of chloroacetophenone for R = H, Cl (entry 5 & 8) but produced a lesser effect for R = -CH₃, -OCH₃ (entries 6 and 7; Figures S27-S30). Eliminating water from the reaction mixture by treating [(TPA)Cu(CH₃CN)](ClO₄)₂ with 2-chloro-1,3-diphenyl-1,3-propanedione and LiHMDS in dry CH₃CN/Et₂O produced no chloroacetophenone (entry 9; Figure S31). However, addition of 200 eq of water to the mixture produced 34% yield of chloroacetophenone (entry 10; Figure S32) providing evidence for the necessity of water for C-C cleavage. Using D₂O (entry 11; Figure S33), *d*₂-2-chloro-1-(phenyl)ethanone was formed, indicating the methylene protons in the product are derived from water. Use of excess MeOH (200 eq; entry 12; Figure S34) instead of water produces 2-chloro-1-(phenyl)ethanone (24%) as well as methyl benzoate (16% yield). This ester represents the cleavage product that is benzoate in the H₂O-mediated retro-Claisen reaction. The discrepancy of the percentage yield between 2-chloro-1-(phenyl)ethanone (bp 244-245 °C) and methyl benzoate (bp 198-200 °C) is related to the higher volatility of the latter.

Table 1. Yield of 2-chloro-1-(4'-R-phenyl)ethanone produced via retro-Claisen reactivity

Entry	Ligand	R	% Yield
1	TPA	H	22(3)
2	TPA	CH ₃	31(3)
3	TPA	OCH ₃	28(1)
4	TPA	Cl	17(2)
5	TPA ^a	H	49(1)
6	TPA ^a	CH ₃	38(2)
7	TPA ^a	OCH ₃	28(2)
8	TPA ^a	Cl	56(4)
9	TPA ^b	H	0
10	TPA ^{a,b}	H	34
11	TPA ^{b,c}	H	40
12	TPA ^{b,d}	H	24 ^e
13	<i>f</i>	H	0
14	<i>g</i>	H	8
15	6-Ph ₂ TPA	H	8(2)
16	BPY	H	13(2)

^a200 eq of H₂O added. ^bThe reaction was performed using [(TPA)Cu^{II}(CH₃CN)](ClO₄)₂. ^c200 eq D₂O added. ^d200 eq MeOH added. ^eMethyl benzoate observed (16%). ^fCu(ClO₄)₂·6H₂O with no supporting chelate ligand. This reaction was worked up using HCl (4 mL, 1M) and CH₂Cl₂ (4 mL) instead of ethyl acetate. ^g2-chloro-1,3-diphenyl-1,3-propanedione in the presence of LiHMDS and water (6 eq) in CH₃CN/Et₂O (1:1).

A control reaction involving no TPA ligand provided evidence that the supporting ligand is required for retro-Claisen reactivity (entry 13; Figure S35). However, treatment of 2-chloro-1,3-diphenyl-1,3-propanedione with LiHMDS and H₂O in absence of Cu(II) and TPA did produce a small amount of 2-chloro-1-(phenyl)ethanone (entry 14). Use of 6-Ph₂TPA or BPY as the supporting chelate ligand produced lower amounts of the retro-Claisen product (entries 15 and 16; Figures S36 and S37) than those found for the TPA-containing systems. Unlike **7-10**, the Cu(II) chlorodiketonate complexes $[(6\text{-Ph}_2\text{TPA})\text{Cu}(\text{PhC}(\text{O})\text{CCIC}(\text{O})\text{Ph})]\text{ClO}_4$ (**1**) and $[(\text{bpy})\text{Cu}(\text{PhC}(\text{O})\text{CCIC}(\text{O})\text{Ph})]\text{ClO}_4$ (**2**) can be isolated in reasonable yields as analytically pure crystalline solids.^{8,9} This is consistent with the lower level of retro-Claisen reactivity in these systems. The chloro substituent on the central carbon is required for the retro-Claisen reactivity, as evidenced by no observed acetophenone production for **3** (Figure S38). Notably, performing the product isolation studies for **7** under O₂ produced only a trace amount of the retro-Claisen product and no oxidative cleavage products (Figure S39). This lack of reactivity necessitates further investigation, but initially indicates that the TPA-ligated complex exhibits notably different reactivity than **1** and **2** in terms of the cleavage of the chlorodiketonate ligand.

Mechanistic Investigations and *In situ* Spectroscopic Studies.

To gain further insight into the dehalogenation and retro-Claisen reactions identified in the reaction mixtures directed at the formation of the TPA-ligated Cu(II) chlorodiketonate complexes, additional mechanistic and spectroscopic investigations were performed. While the dehalogenation product in the reactions of **7-10** was not quantified, it appears in higher amounts in the organic recovery of reaction mixtures containing excess water. Organic dehalogenation reactivity is known for TPA-ligated Cu(I) complexes to give $[(\text{TPA})\text{Cu}(\text{II})\text{-Cl}]^+$ salts.²⁶⁻²⁸ We found that mixing $[(\text{TPA})\text{Cu}(\text{CH}_3\text{CN})]\text{PF}_6$ with 2-chloro-1,3-diphenyl-1,3-propanedione in CH₃CN results in dehalogenation (Scheme S1; Figures S40-S41). Maximum yield is obtained using two equivalents of $[(\text{TPA})\text{Cu}(\text{CH}_3\text{CN})]\text{PF}_6$ consistent with the two-electron reduction of 2-chloro-1,3-diphenyl-1,3-propanedione to 1,3-diphenyl-1,3-propanedione. Based on these studies, dehalogenation reactivity could result from reduction of *in situ* generated $[(\text{TPA})\text{Cu}(\text{CH}_3\text{CN})](\text{ClO}_4)_2$ in CH₃CN to give $[(\text{TPA})\text{Cu}(\text{CH}_3\text{CN})]^+$ which mediates the dehalogenation. However, at this time, we cannot identify the reducing agent for Cu(II) in the system.

We next investigated the reaction mixture of **7** as a function of time using EPR. Aliquots for EPR studies were removed after 1 and 48 h of stirring at ~30 °C, respectively. Each sample was brought to dryness under reduced pressure, dissolved in CH₃CN/toluene (1:1) and subsequently frozen in liquid N₂. Spectra collected at 12 K are shown in Figure 3. At least two species are present, with one having g values ($g_{\parallel} > g_{\perp}$) similar to **3-6**. This may be $[(\text{TPA})\text{Cu}(\text{PhC}(\text{O})\text{CCIC}(\text{O})\text{Ph})]\text{ClO}_4$ (**7**) or its dehalogenation product $[(\text{TPA})\text{Cu}(\text{PhC}(\text{O})\text{CHC}(\text{O})\text{Ph})]\text{ClO}_4$ (**3**). The cations of both species were detected by ESI-MS.

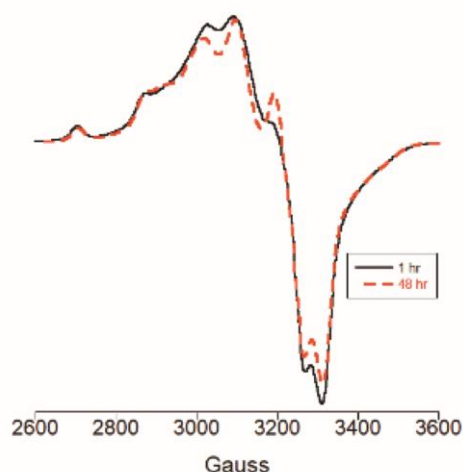


Figure 3. EPR spectra of aliquots from the reaction mixture of **7** after stirring for 1 hr (black) and 48 hr (red) at 30 °C. The samples were collected in CH₃CN:toluene (1:1) at 12 K. For the first product, $g_{\parallel} = 2.27$, $g_{\perp} = 2.08$.

Additional species that may be present based on ESI-MS could be $[(\text{TPA})\text{CuCl}]^+$ or $[(\text{TPA})\text{Cu}(\text{O}_2\text{CPh})]^+$. An independently prepared sample of $[(\text{TPA})\text{Cu}(\text{O}_2\text{CPh})]\text{ClO}_4$ (**12**) (Figure S42) exhibited EPR features consistent with a trigonal bipyramidal Cu(II) center with $g_{\perp} > g_{\parallel}$ and an unpaired electron in the d_{z^2} orbital. Contributions from such a species are suggested by the EPR spectral features observed after 48 h for reaction mixtures involving **8** and **9**. (Figures S43 and S44) The EPR features for **10** (Figure S45) are similar to those of **7**.

Absorption spectra of the reaction mixture involving **7** were collected at 1, 24 and 48 h. These features were compared to those of analytically pure **3** dissolved in CH₃CN. A $\pi\text{-}\pi^*$ band is present at 351 nm for the reaction mixture for **7** (Figure S46), after 1 h which is slightly blue-shifted compared to the $\pi\text{-}\pi^*$ band of **3** (356 nm). This feature indicates the formation of diketonate complexes in the solution of **7** and changes

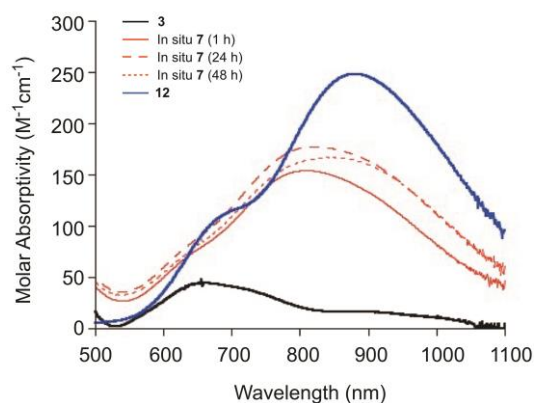
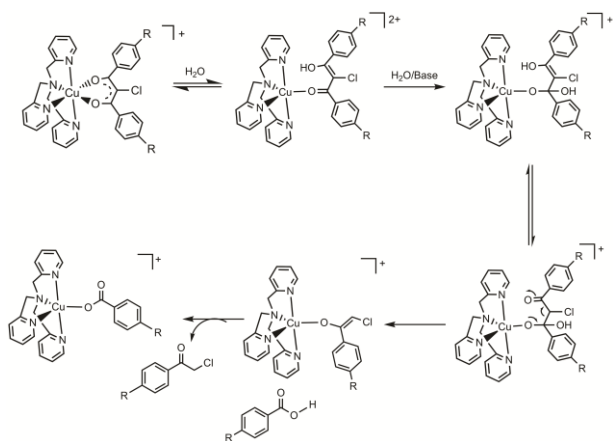


Figure 4. Absorption spectral features of **3**, in situ **7** at 1, 24 and 48 h, and $[(\text{TPA})\text{Cu}(\text{O}_2\text{CPh})]\text{ClO}_4$ (**12**) in CH₃CN.

minimally over time. The *d-d* region for **7** after 1, 24 and 48 h was also examined and compared to that of **3** (Figure 4) and the benzoate complex **12**. An enhanced *d-d* absorbance at ~850 nm in the reaction mixture of **7** at 1 h suggests the possible formation of a mixture that includes trigonal bipyramidal Cu(II) species in solution. This assessment is based on spectral comparison to the features for [(TPA)CuCl]Cl (*d-d* absorption ~855 nm) and [(TPA)Cu(O₂CPh)]⁺ (*d-d* absorption ~876 nm).^{29,30} Notably, organic product recovery at 1 h (Figure S47) indicates minimal dehalogenation or retro-Claisen reactivity has occurred to that point. This suggests changes in the geometry of the Cu(II) center prior to anaerobic C-C and C-X bond cleavage. After 48 h, when organic dehalogenation and retro-Claisen products have been formed, the presence of the ~850 nm absorption feature is consistent with the formation of [(TPA)CuCl]⁺ and [(TPA)Cu(O₂CPh)]⁺ (**12**), which is supported by the ESI-MS and EPR data.

Proposed Mechanism for Retro-Claisen Reactivity. Based on the structural features of **3-6** and the in situ spectroscopic studies, a proposed mechanism for retro-Claisen reactivity in **7-10** is shown in Scheme 5. Initiation of the reaction could occur with protonation of the chlorodiketonate by water, leading to the formation of a five-coordinate species which subsequently undergoes nucleophilic addition of OH⁻ (derived from base and H₂O in the reaction mixture) leading to retro-Claisen cleavage and formation of **12**. We hypothesize that the difference in anaerobic retro-Claisen reactivity between TPA- and 6-Ph₂TPA or BPY-ligated Cu(II) complexes relates to the propensity of the TPA-ligated systems, due to steric effects, to promote monodentate coordination of the neutral diketone ligand. This results from the higher coordination number of the TPA supporting chelate ligand versus 6-Ph₂TPA and BPY.



Scheme 5. Proposed mechanism of retro-Claisen reactivity in **7-10**.

Conclusions

In summary, we report the preparation and characterization of the first examples of TPA-ligated Cu(II) diketonate complexes. We have found that Cu(II) chlorodiketonate derivatives exhibit

anaerobic retro-Claisen type C-C bond cleavage reactivity which exceeds that of analogs supported by chelate ligands with fewer and/or weaker pyridyl interactions. These studies demonstrate that the number of pyridyl donors surrounding a Cu(II) center influences diketonate reactivity and therefore should be a factor considered in reactions involving Cu(II) salt-mediated diketonate cleavage reactivity.

Acknowledgements

We thank the National Science Foundation (CHE-1664977 to LMB; CHE-1429195 for Brüker Avance III HD 500 MHz NMR; CHE-1828764 for Rigaku Benchtop XtaLAB Mini II X-ray diffractometer). X-ray crystallographic studies of **3**, **4**, **11** and **12** were performed at the University of Montana (NIH, COBRE NIGMS P20GM103546). Single crystal X-ray diffraction data were collected using a Bruker D8 Venture (NSF MRI CHE-1337908). We would also like to thank Dr. Zhiyong Yang for his assistance with the collection of EPR data.

Conflicts of interest

The authors declare no conflict of interest

References

- Y-F. Liang, N. Jiao, *Acc. Chem. Res.*, 2017, **50**, 1640-1653.
- C. J. Allpress, L. M. Berreau, *Coord. Chem. Rev.*, 2013, **257**, 3005-3029.
- C. Zhang, P. Feng, N. Jiao, *J. Am. Chem. Soc.*, 2013, **135**, 15257-15262.
- C. Zhang, X. Wang, N. Jiao, *Synlett*, 2014, **25**, 1458-1460.
- M. Jukic, D. Sterk, Z. Casar, *Curr. Org. Syn.*, 2012, **9**, 488-512.
- L-H. Zhou, D. L. Priebbenow, L. Wang, J. Mottweiler, C. Bolm, *Adv. Synth. Catal.*, 2013, **355**, 2558-2563.
- K. Uehara, F. Kitamura, M. Tanaka, *Bull. Chem. Soc. Jpn.*, 1976, **49**, 493-498.
- C. J. Allpress, A. Milaczewska, T. Borowski, J. R. Bennett, D. L. Tierney, A. M. Arif, L. M. Berreau, *J. Am. Chem. Soc.*, 2014, **136**, 7821-7824.
- S. L. Saraf, A. Milaczewska, T. Borowski, C. D. James, D. L. Tierney, M. Popova, A. M. Arif, L. M. Berreau, *Inorg. Chem.*, 2016, **55**, 6916-6928.
- B. G. Williams, M. Lawton, *J. Org. Chem.*, 2010, **75**, 8351-8354.
- Z. Tyeklár, R. R. Jacobson, N. Wei, N. N. Murthy, J. Zubieta, K. D. Karlin, *J. Am. Chem. Soc.*, 1993, **115**, 2677-2689.
- M. M. Makowska-Grzyska, E. Szajna, C. Shipley, A. M. Arif, M. H. Mitchell, J. A. Halfen, L. M. Berreau, *Inorg. Chem.*, 2003, **42**, 7472-7488.
- A. Hu, W. Lin, *Org. Lett.*, 2005, **7**, 455-458.
- Z. S. Zhou, L. Li, X. H. He, *Chin. Chem. Lett.*, 2012, **23**, 1213-1216.
- J. Wang, M. P. Schopfer, S. C. Puiu, A. A. N. Sarjeant, K. D. Karlin, *Inorg. Chem.*, 2010, **49**, 1404-1419.
- W. C. Wolsey, *Chem. Ed.*, 1973, **50**, 335-337.
- G. M. Sheldrick, *SADABS: Area Detector Absorption Correction*, University of Göttingen, Germany, 1996.
- O. V. Dolomanov, L. J. Bourhis, R. J. Gildea, J. A. K. Howard, H. Puschmann, *J. Appl. Crystallogr.*, 2009, **42**, 339-341.

- 19 G. M. Sheldrick, *Acta Crystallogr.*, 2015, **A71**, 3–8.
- 20 G. M. Sheldrick, *Acta Crystallogr.*, 2015, **C71**, 3–8.
- 21 Bruker, *APEX2*, Bruker AXS Inc., Madison, Wisconsin, USA, 2007.
- 22 Bruker, *APEX3*, Bruker AXS Inc., Madison, Wisconsin, USA, 2016.
- 23 CrysAlisPro, Rigaku Oxford Diffraction, version 171.40.67a, 2019.
- 24 I. J. Bruno, J. C. Cole, M. Kessler, J. Luo, W. D. S. Motherwell, L. H. Purkis, B. R. Smith, R. Taylor, R. I. Cooper, S. E. Harris, A. G. Orpen, *J. Chem. Inf. Comput. Sci.*, 2004, **44**, 2133-2144.
- 25 C. F. Macrae, P. R. Edgington, P. McCabe, E. Pidcock, G. P. Shields, R. Taylor, M. Towler, J. van de Streek, *J. Appl. Cryst.*, 2006, **39**, 453-457.
- 26 W. Tang, K. Matyjaszewski, *Macromolecules*, 2006, **39**, 4953-4959.
- 27 B. Lucchese, K. J. Humphreys, D-H. Lee, C. D. Incarvito, R. D. Sommer, A. L. Rheingold and K. D. Karlin, *Inorg. Chem.*, 2004, **43**, 5987-5998.
- 28 D. Maiti, A. A. N. Sarjeant, S. Itoh, K. D. Karlin, *J. Am. Chem. Soc.*, 2008, **130**, 5644-5645.
- 29 H. Zheng, L. Que, Jr., *Inorg. Chim. Acta* 1997, **263**, 301-307.
- 30 M. R. Malachowski, H. B. Huynh, L. J. Tomlinson, R. S. Kelly, J. W. Furbee jun., *J. Chem. Soc. Dalton Trans.*, 1995, **1**, 31-36.